

# Graphene oxide nanosheets decorated with Gold-Silver core-shell using pulsed laser ablation technique

*Mira Tawfik<sup>1\*</sup>, A. Khalid<sup>1</sup>, S. Abdallah<sup>1</sup> and S. Negm<sup>1</sup>*

<sup>1</sup> *Laser physics & technology unit (LPTU), Department of Basic Engineering Sciences, Faculty of Engineering at Shoubra, Benha University, Cairo, Egypt*

## Abstract

Gold-silver (Au-Ag) core-shell nanocomposites were successfully synthesized via pulsed laser ablation (PLA). Similarly, graphene oxide (GO) nanosheets were prepared from graphite in pure distilled water via (PLA) technique. GO nanosheets were decorated with (Au-Ag) core-shell by mixing 10 ml of (Au-Ag) with 20 ml of GO. The loading of the core-shell and the morphology of (Au-Ag) on the GO were examined using Transmission Electron Microscopy (TEM) which showed that the (Au-Ag) core-shell was decorated on a GO sheet. Electron Diffraction X-ray (EDX) was used to determine the percentage of the decoration in the prepared samples. The GO sheets and deposition of (Au-Ag) core-shell on GO were also analyzed using UV-visible absorption spectra. These results revealed that (Au-Ag) @GO has all the characterization peaks of the GO and (Au-Ag) core-shell. Using the optical absorption spectra, the absorption coefficient ( $\alpha$ ), refractive index ( $n$ ), and optical conductivity ( $\sigma_{opt}$ ) were calculated for the prepared samples which increased by adding (Au-Ag) to the GO sheet. The optical properties of (Au-Ag) @GO make it an excellent candidate for photonic applications.

## Keywords

Graphene oxide GO, Gold-Silver core-shell Au-Ag nanoparticles, laser ablation technique.

\*: [mira.tawfik@feng.bu.edu.eg](mailto:mira.tawfik@feng.bu.edu.eg)

Receive Date: 24-9-2024; Revise Date: 15-10-2024; Accept Date: 17-10-2024; Publish: 17-10-2024

## 1. Introduction

Because graphene, for instance, contains a single sheet of sp<sup>2</sup> hybridized carbon atoms densely packed into a 2D honeycomb crystal lattice, it was also considered to be a unique type of 2D material [1, 2]. Its remarkable qualities, such as its greater electrical, thermal, and mechanical facilities, high surface area, and intricate surface features, have attracted the attention of the scientific community [3–5]. The zero-band gap classification of graphene as a semiconductor restricts its use in photonics, optoelectronics, photodetectors, and photovoltaic energy storage [6]. To increase the spectrum of applications and enhance graphene's qualities, Graphene sheets have been successfully decorated with a range of nanoparticles. Some researchers have already adsorbed SnO<sub>2</sub> on graphene to produce a SnO<sub>2</sub>-graphene composite with enhanced photovoltaic performance [7]. By catalytically creating TiO<sub>2</sub>-graphene nanocomposites, Cheng et al. enhanced the catalytic properties of graphene [8].

There has been a lot of interest in the integration of GO with Nobel metals (NPs), like Ag and Au [9–11]. Special characteristics including optical, biological, and thermal issues made these attempts challenging [12–13]. As a highly efficient and broad-spectrum bactericide, (Au-Ag) nanocomposites have been used. The (Au-Ag) @GO nanocomposite can reduce the recombination of electron-hole pairs to increase its photocatalytic activity. In biomedical applications, the (Au-Ag) is unique because of surface plasmon resonance (SPR), which is highly reliant on nanoparticles (NPs), especially as an anti-tumorigenic and antibacterial agent. It also effectively absorbs light within the visible spectrum [14]. Many people effectively decorated (metal or metal oxide) on graphene sheets and examined the features of these unique nanocomposites. A.R. Sadrolheseini et al. synthesized Silver Nanoparticles in Graphene Oxide and the Thermal effectivity of nanocomposite [11]. Jin et al. described how Pd nanoparticles are formed and adhered to thermally exfoliated graphene sheets suspended in a solvent in situ, therefore decorating the graphene sheets [15]. Gaboardi et al. developed a two-step, oxygen- and water-free chemical procedure to create nickel-decorated thermally exfoliated graphene oxide [16]. Khalid et al. used a low-temperature hydrothermal technique to adorn graphene sheets

after synthesizing nitrogen-doped TiO<sub>2</sub> Nanoparticles via the sol-gel method [17].

One of the most effective, stable, and sustainable methods for creating nanostructure materials is pulsed laser ablation. , the process's relative simplicity, and the lack of chemical reagents, which can be hazardous and detrimental to applications. The basis of this method is the generation of laser pulse trains within any liquid medium [18-19].

The development of novel, efficient materials with improved properties is essential, since research on optical material applications is still in its early stages [20]. Improving optical properties (optical band gap and refractive index) is the main goal of assessing optoelectronic materials [21].

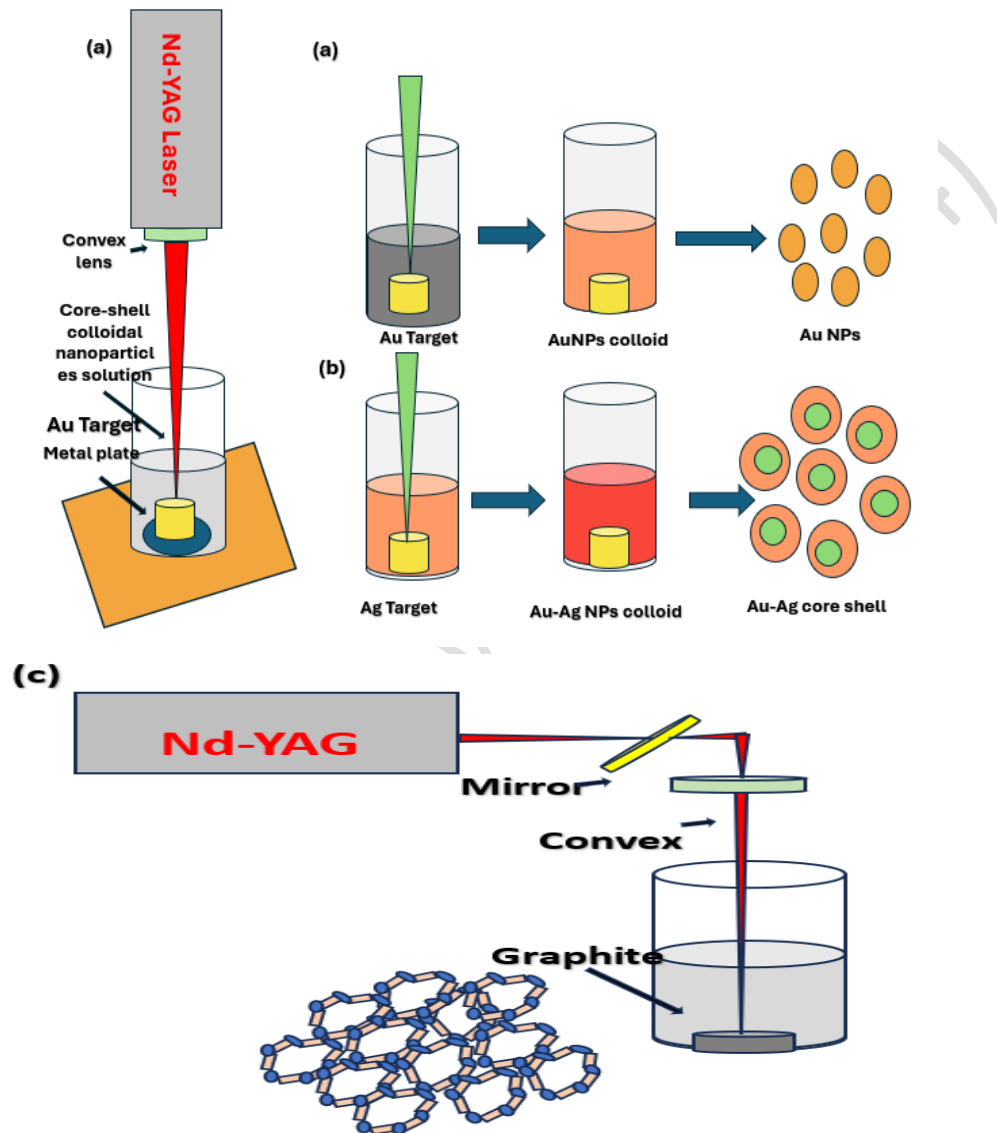
To investigate structural and optical properties, we decorated GO with (Au-Ag) nanocomposites to produce (Au-Ag) @GO in this work. The primary goals of this work are to synthesize (Au-Ag) nanocomposites and examine how GO influences their structure and optical characteristics. (Au-Ag) and (Au-Ag) @GO nanocomposite were investigated via, EDX, TEM, and UV-visible spectroscopy.

## 2. Experimental

### 2.1. Synthesis of (Au-Ag) @GO Nanocomposites

We employed a very pure gold (Au) and silver (Ag) metal plate in our investigation. (cleanliness 99.99% according to Sigma Aldric) thickness of 2 mm, which was employed to create the (Au-Ag) core-shell by the laser ablation method [11,19]. The Au rod was fixed at the bottom of 30ml of distilled water and focused by the Q-Switched Nd: YAG (Quanta-Ray) laser beam pulsed for five minutes, each pulse lasting eight nanoseconds, As shown in Fig. 1a, a lens with a focal length of 20 cm was used to focus light at a wavelength of 1064 nm and with a frequency of 10 Hz on the surface of the Au target [22]. The target was sterilized for 30 minutes in an ultrasonic bath, afterward sanitized with ethanol and distilled water, and then fixed 18 mm below the distilled water surface. A target with a thickness of 2 mm was put on the bottom of a vessel, including 30 ml of distilled water. Then, the Ag plate was immersed into 30 ml of Au NPs solution and irradiated by

Laser as seen in Fig. 1b. At the ambient temperature, the ablation procedure was performed and (Au-Ag) Nanocomposites were formed after 80 minutes.



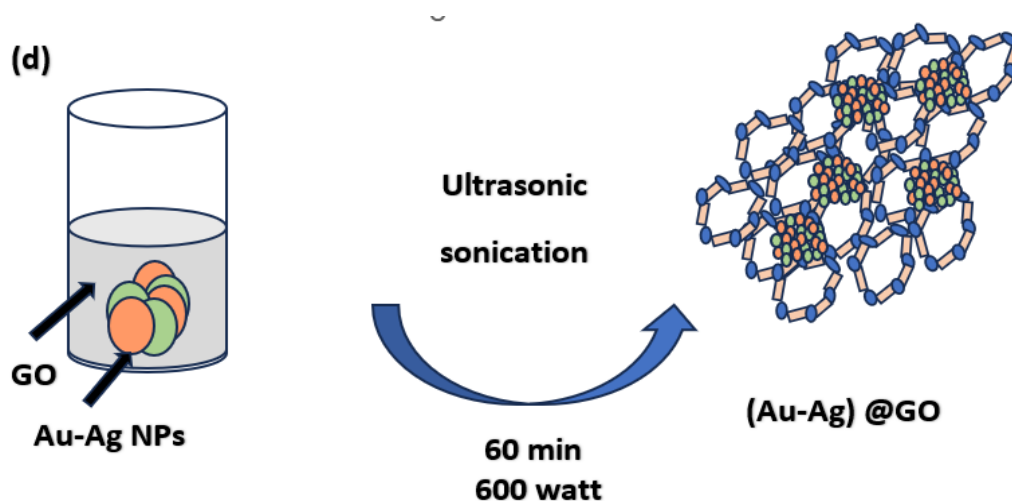


Fig. 1. Schematic set-up for laser ablation of (a) (Au) NPs, (b) (Au-Ag) core-shell, (c) GO sheet, and (d) (Au-Ag) @GO nanocomposites

Fig.1c shows the Incident laser on the graphite target. GO was prepared using the same production from graphite target and the production of nanosheets in distilled water was confirmed by observing a change in color during the ablation process [23].

The (Au-Ag) @GO nanocomposites were prepared by mixing 10 ml of (Au-Ag) with 20 ml GO in DI water, then probe sonicated for 60 min at 600 Watt. Finally, the obtained (Au-Ag)@ GO nanocomposites were dispersed in distilled water as seen in Fig. 1d.

## 2.2. Characterization Techniques

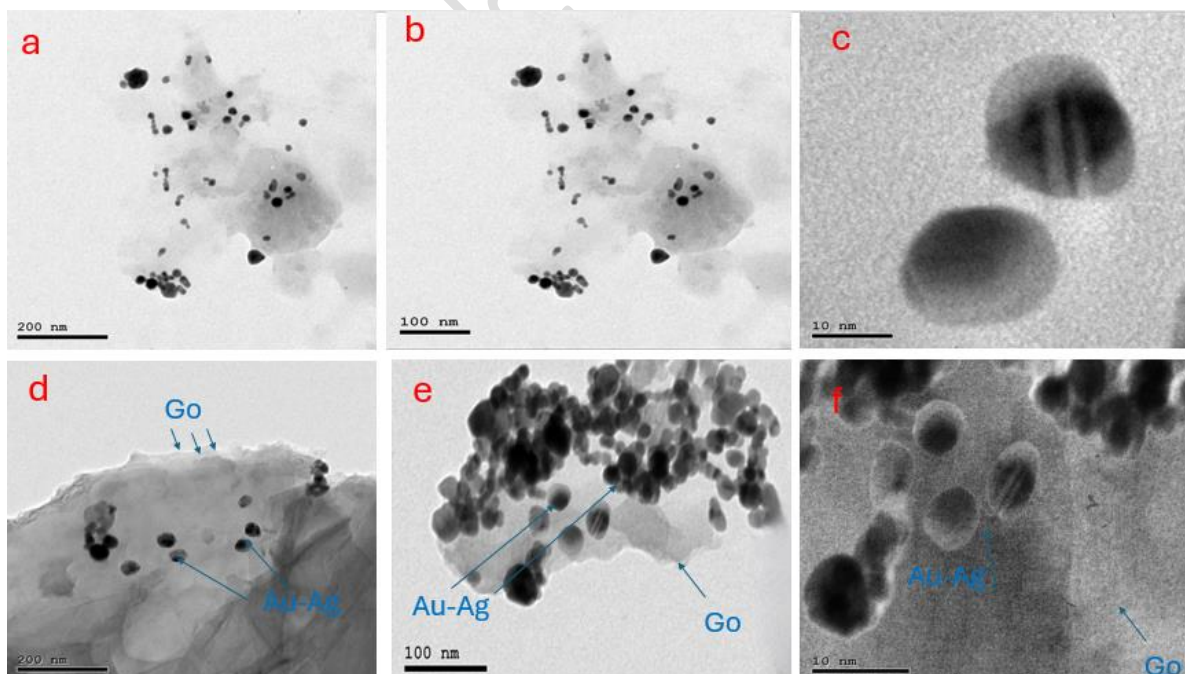
A transmission electron microscope (TEM), model Joel-JEM-2100, operating at 200 kV, was used to determine the TEM images of the materials. Using a twin beam spectrophotometer (JASCO -670), the materials' UV-Vis absorption spectra were determined. The JOEL -JSM Model 5600 Energy Dispersive X-ray (EDX)

### 3. Results

#### 3.1. TEM Analysis and EDX

The (Au-Ag) and (Au-Ag) @GO nanocomposite samples were analyzed by TEM examination at different magnifications, as illustrated in Fig. 2. to determine the particle size and shape.

Fig.2(a-c) shows (Au-Ag) core-shell in a semi-spherical morphology with an around average particle size  $\sim$ of 22.4 nm. The main cause of nanoparticle agglomeration is the combination of small and high surface energy particles. Fig 2. (d-f) illustrates the (Au-Ag)@GO hybridization composite's TEM picture.; The two-dimensional graphene oxide (GO) sheets decorated with (Au-Ag) comprise the hybrid nanocomposites. It illustrates that a sizable portion of (Au-Ag) have the regular shape of spheres and within the range size of 18.4 nm are decorated on GO sheet which acts as a stage. Furthermore, from the particle size distribution, Fig.2(g,h), the average particle sizes are 22.4 nm for (Au-Ag) and 18.4 nm for (Au-Ag) @GO. The (Au-Ag) growth is impeded by the GO sheet, and the size of the particles also gets smaller. This is consistent with the literature[24,25].



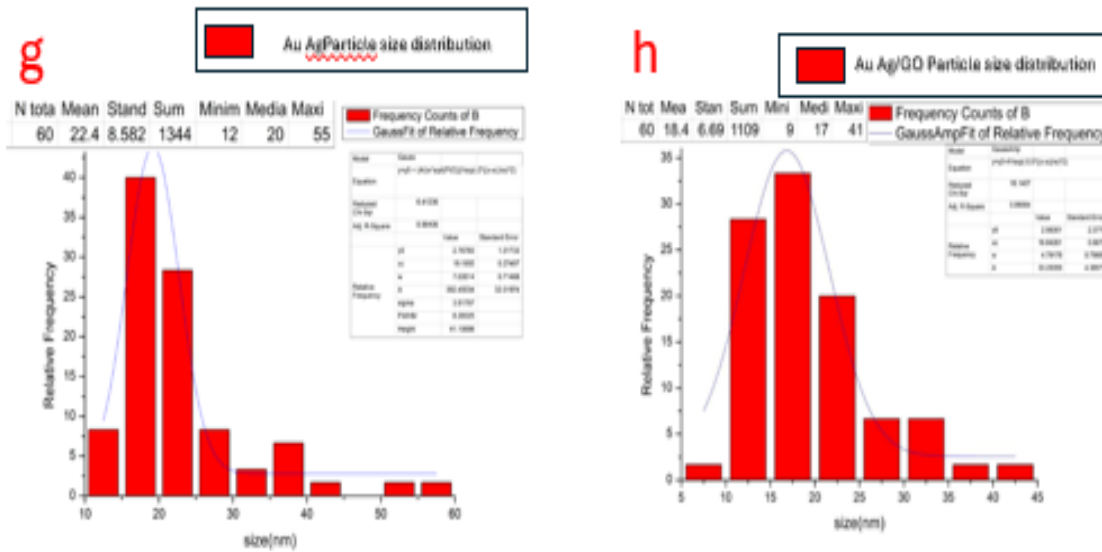


Fig. 2. TEM images and histogram (Au-Ag) and (Au-Ag)@GO.

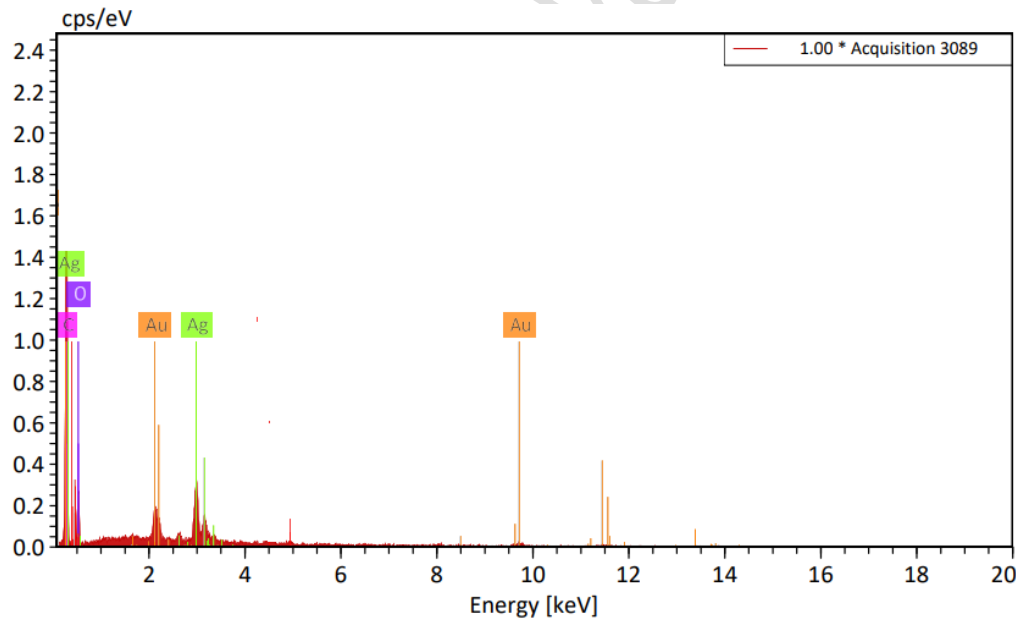


Fig. 3. EDX of (Au-Ag) @GO nanocomposites

To confirm the existence of (Au-Ag) in the GO sheet, Fig. 3 displays the outcomes from the EDX analysis. of (Au-Ag) @GO nanocomposites. It displays the ratios of the elements carbon (C), oxygen (O), gold (Au), and silver (Ag), where the GO is denoted by the elements C and O.

### 3.2. Optical properties

Fig. 4 illustrates the absorption spectra of the (Au-Ag) and (Au-Ag)@GO samples.

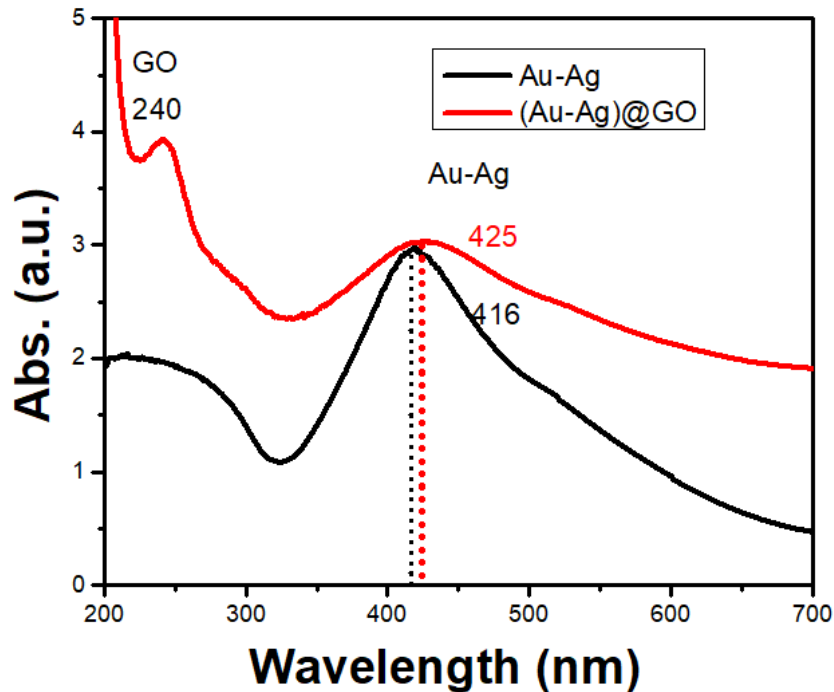


Fig. 4. The absorption spectra for the synthetic samples' (Au-Ag) and (Au-Ag)@GO

The UV-visible absorption bands of the samples are displayed in Fig.4. Clear absorption bands are seen for (Au-Ag)@GO at 240 nm and 425 nm, which correlate with the (Au-Ag) core-shell and GO ( $n-\pi^*$  (C=O bonds) transitions, respectively[23,26]. As shown the absorption edge located in the visible region, which indicated the lower bandgap value of the prepared samples. Adding the GO to the (Au-Ag) core-shell clearly causes the absorption spectra to rise and shift toward longer wavelengths. The addition of GO to the (Au-Ag) matrix results in the redshift at the absorption edge. Because graphene has great electron mobility and restricts the recovery of electron holes, The absorption efficiency of the (Au-Ag) core-shell was improved by the use of graphene [1]. Furthermore, the GO increases the (Au-Ag) visible light activity. Due to the GO sheets, the (Au-Ag) composite is



able to increase energy absorption in the UV-visible range, It is beneficial for solar panels and other optical applications[28].

In the visible region, clearly  $\lambda_c$  is about 416 nm and 425 nm for (Au-Ag) and (Au-Ag) @GO composites, respectively. The following formula was used to determine the optical bandgap  $E_g$ ,  $E_g=1240/\lambda_{max}$ . The  $E_g$  values are 2.981 eV and 2.917 eV for (Au-Ag) and (Au-Ag) @GO, respectively. A reduction in  $E_g$  corresponds to the localized states generated in the restricted region as a result of GO sheet flaws [28]. Optical band gap may have changed because of the irregular distribution of flaws in GO sheets, which results in irregular distribution in sp<sup>2</sup> carbon islands[24,29].

Fig. 5a illustrates the relationship between the wavelength and the extinction coefficient. The extinction coefficient ( $K=\alpha\lambda/4\pi$ ) is calculated as ( $\alpha =2.302\lambda/x$ ) and x is the thickness of the plate which we used 1cm. Furthermore, the material coefficient (K) increases as a result of the proportional relationship with the absorption coefficient[2].

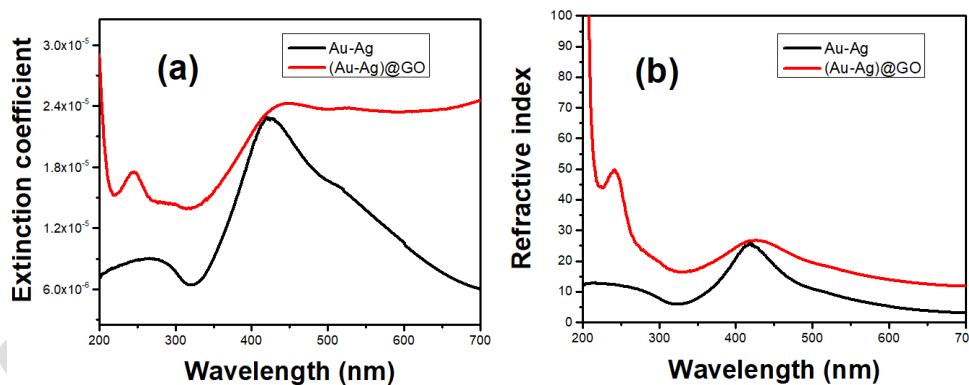


Fig.5. Graphs of Extinction coefficient (a) and refractive index (b) vs. the wavelength for the synthesized (Au-Ag) and (Au-Ag) @GO samples.

It is clear that adding GO sheets to the matrix decreases the amount of light lost through scattering and also raises the extinction coefficient. In

addition to this, the material's reflectivity index rises according to its density, which reduces the amount of light it transmits and increases the amount of light it scatters. Fig. 5b displays the relationship among the refractive index against the light wavelength for (Au-Ag) and (Au-Ag) @GO. The refractive index provides a useful tool for industrial applications by indicating a material's reflection. As previously mentioned, when GO is added to the matrix, the material's refractive index rises. The size of the crystallites decreases, the surface area grows, and the density likewise rises when the GO gets mixed into the (Au-Ag). As the consequence, both the material's reflectivity and refractive index increase [2].

One fundamental property of the material is the complex dielectric constant, and it consists of two parts.: real ( $\epsilon'$ ) imaginary ( $\epsilon''$ ), as the equation shows which below [21]

$$\epsilon = \epsilon' + i\epsilon'' \dots \dots$$

The real part ( $\epsilon'$ ) shows how light is distributed throughout the material, and the imagined part ( $\epsilon''$ ) shows how energy is absorbed due to its motion of the dipole moment [21],

$$\epsilon' = n^2 - k^2$$

$$\epsilon'' = 2nk$$

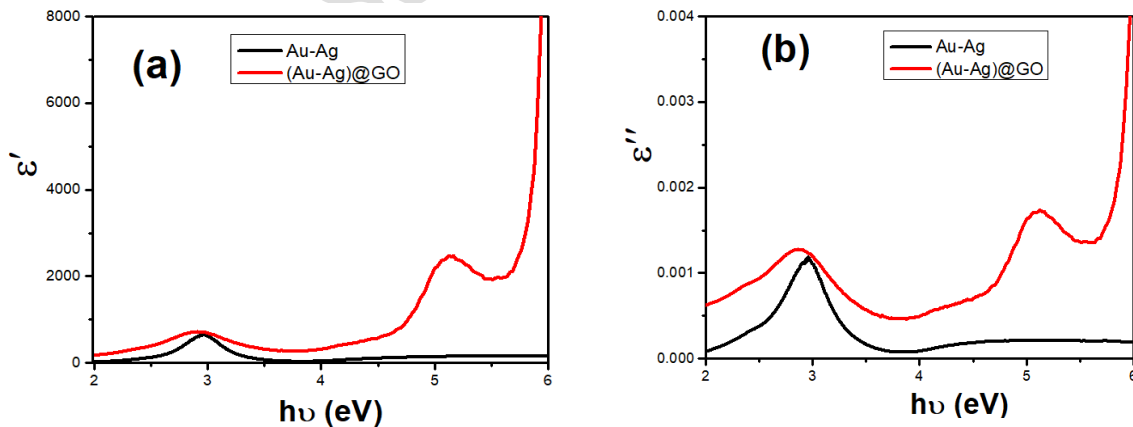


Fig .6. Graphs of (a)  $\epsilon'$  and (b)  $\epsilon''$  vs.  $h\nu$  for the synthesized (Au-Ag) and (Au-Ag) @GO samples.

Fig. 6 shows how both variables  $\epsilon'$  and  $\epsilon''$ , depend on the incident photon energy. It is evident that when the GO additions to the (Au-Ag) nanocomposite grow, so do  $\epsilon'$  and  $\epsilon''$

It is clear that the behaviour of the  $\epsilon'$  with refractive index and the  $\epsilon''$  with  $k$  are comparable.

Also, the value is higher than that of  $\epsilon''$ . Growing the GO additives to the Au-Ag nano composite leads to a shift in polarization, which reduces the distribution of energy and produces high  $\epsilon'$  and low  $\epsilon''$  values.

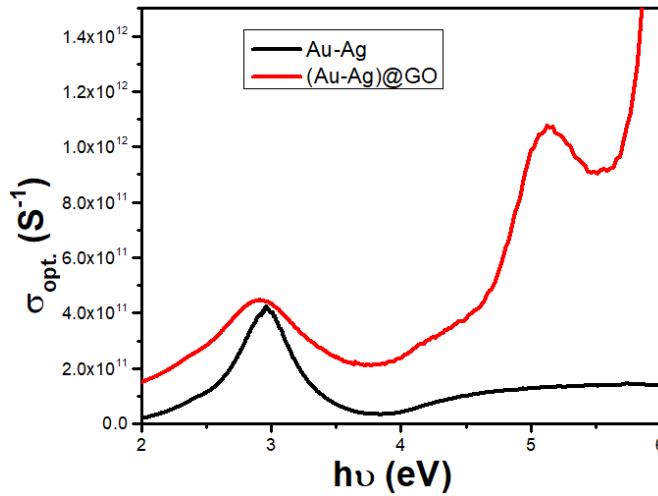


Fig.7. The variation of  $\sigma_{opt}$ , with  $(h \nu)$  for the synthesized (Au-Ag) and (Au-Ag) @GO samples.

A material's optical conductivity ( $\sigma_{opt}$ ) indicates how the induced current density affects the electric field produced at random frequencies [3]. Electron excitation is produced by the motion of free charge carriers as a result of the electromagnetic photon beam, which starts optical conductivity.

Moreover, this parameter can be calculated using the relationship that follows[3,4].

$$\sigma_{opt} = \frac{n\alpha c}{4\pi}$$

where  $(c=3 \times 10^8 \text{ m/sec})$  is the speed of light in free space. The relationship between  $\sigma_{opt}$ . And the energy of incoming photons is seen in Fig. 7.

It is evident that the  $\sigma_{opt}$  grows as the GO additions to the (Au-Ag) composite increase. This could be because of the rise in  $\alpha$  and  $n$  values of the material with added GO to the (Au-Ag) composite. The excitation of electrons by incident photons results in increased optical conductivity at high photon energy.

### Conclusion:

(Au-Ag) core-shell and GO sheets were successfully synthesized by pulsed laser ablation (PLA) technique. The (Au-Ag) @GO nanocomposites were prepared by mixing (Au-Ag) with GO in DI water. TEM analysis showed that the (Au-Ag) core shell was decorated on a GO sheet. EDX was used to determine the percentage of the decoration in the prepared samples. The comprehensive analyses conducted showcased the influence of GO sheets on the structure of (Au-Ag) nanocomposites and their optical parameters. The size of the (Au-Ag) core-shell is decreased from 22.4 nm to 18.4 nm due to the GO sheet which hindered the growth of the (Au-Ag) core-shell. The absorption coefficient ( $\alpha$ ), refractive index ( $n$ ), and optical conductivity ( $\sigma_{opt}$ ) increased by adding (Au-Ag) to the GO sheet. The observed band gap aligns well with the range of the Solar System. Finally, it can be said that (Au-Ag) @GO nanocomposites are an ideal candidate for many uses, such as solar cells.

### References:

1. Novoselov KS, Fal'ko VI, Colombo L, Gellert PR, Schwab MG, Kim K, A roadmap for graphene. *Nature*. 2012, 11;490(7419):192-200. Doi: 10.1038/nature11458.
2. Zhao, M. Direct Synthesis of Graphene Quantum Dots with Different Fluorescence Properties by Oxidation of Graphene Oxide Using Nitric Acid. *Appl. Sci*. 2018, 8, 1303. <https://doi.org/10.3390/app8081303>
3. Maria-Hormigos R, Jurado-Sánchez B , Escarpa A , Graphene quantum dot based micromotors: a size matter. *Chem Commun (Camb)*. 2019 Jun 6;55(47):6795-6798. Doi: 10.1039/c9cc02959a.
4. Avouris P. Graphene: electronic and photonic properties and devices. *Nano Letters*. 2010 Nov;10(11):4285-4294. Doi: 10.1021/nl102824h.

5. Chen D, Tang L, Li J. Graphene-based materials in electrochemistry. *Chem Soc Rev.* 2010, 39(8):3157-80. Doi: 10.1039/b923596e.
6. T.A. Tabish, S Zhang, Graphene Quantum Dots: Syntheses, Properties, and Biological Applications, *Comprehensive Nanoscience and Nanotechnology (Second Edition)*, 2016, 171-192, ISBN 9780128122969, <https://doi.org/10.1016/B978-0-12-803581-8.04133>
7. Guo, Qi & Zheng, Zhe & Gao, Hailing & Ma, Jia & Qin, Xue, SnO<sub>2</sub>/graphene composite as highly reversible anode materials for lithium-ion batteries. *Journal of Power Sources*, (2013). 240. 149–154, doi/10.1016/j.jpowsour.2013.03.116.
8. Ping Cheng, Zhi Yang, Hong Wang, Wei Cheng, Mingxia Chen, Wenfeng Shangguan, Guifu Ding, TiO<sub>2</sub>-graphene nanocomposites for photocatalytic hydrogen production from splitting water, *International Journal of Hydrogen Energy*, 37, 3, 2012, 2224-2230, <https://doi.org/10.1016/j.ijhydene.2011.11.004>.
9. Miao P, Tang Y, Wang L. DNA Modified Fe<sub>3</sub>O<sub>4</sub>@Au Magnetic Nanoparticles as Selective Probes for Simultaneous Detection of Heavy Metal Ions. *ACS Appl Mater Interfaces.* 2017, 1;9(4):3940-3947. doi: 10.1021/acsami.6b14247.
10. Ventrappagada, Lakshman & R. S., Sai Siddhardha & Kaniyoor, Adarsh & Podila, Ramakrishna & Molli, Muralikrishna & Kumar, Sai & Kamiseti, Venkataramaniah & Sundara, Ramaprabhu & Rao, A. & Ramamurthy, Sai. Gold Decorated Graphene by Laser Ablation for Efficient Electrocatalytic Oxidation of Methanol and Ethanol. *Electroanalysis.* (2014). Doi: 10.1002/elan.201400244.
11. A. R. Sadrolhousseini et al., Laser ablation synthesis of silver nanoparticle in graphene oxide and thermal effusivity of nanocomposite, 2013 IEEE 4th International Conference on Photonics (ICP), Melaka, Malaysia, 2013, pp. 62-65, doi: 10.1109/ICP.2013.6687068.
12. Muidh Alheshibri, Khaled Elsayed, Shamsuddeen A. Haladu, Saminu Musa Magami, Abbad Al Baroot, İsmail Ercan, Filiz Ercan, Abdullah A. Manda, Emre Çevik, T.S. Kayed, Aamerah A Alsanea, Amjad Mujawwil Alotaibi, Amal L. Al-Otaibi, Synthesis of Ag nanoparticles-decorated on CNTs/TiO<sub>2</sub> nanocomposite as efficient photocatalysts via nanosecond pulsed laser ablation, *Optics & Laser Technology*, V155, 2022, 108443, ISSN 0030-3992, <https://doi.org/10.1016/j.optlastec.2022.108443>.

13. Qayyum, Hamza & Amin, Said & Ahmed, Waqqar & Mohamed, Tarek & Urrehman, Zia & Hussain, Shafqat. Laser-based two-step synthesis of Au-Ag alloy nanoparticles and their application for surface-enhanced Raman spectroscopy (SERS) based detection of rhodamine 6G and urea nitrate. *Journal of Molecular Liquids*. 365. 2022, Doi 120120. 10.1016/j.molliq.2022.120120.
14. Hoda Aleali, Leila Sarkhosh, Mina Eslamifar, Rouhollah Karimzadeh and Nastaran Mansour. Thermo-Optical Properties of Colloids Enhanced by Gold Nanoparticles. 2010 The Japan Society of Applied Physics Japanese Journal of Applied Physics, V 49, Number 8R 2010 Jpn. J. Appl. Phys. Doi 10.1143/JJAP.49.08500
15. Jin, Zhong & Nackashi, David & Lu, Wei & Kittrell, Carter & Tour, James, Decoration, Migration, and Aggregation of Palladium Nanoparticles on Graphene Sheets. *Chemistry of Materials*. 2010, Doi 22. 10.1021/cm102187a.
16. Gaboardi, Mattia and Bliersbach, Andreas and Bertoni, Giovanni and Aramini, Matteo and Vlahopoulou, Gina and Pontiroli, Daniele and Mauron, Philippe and Magnani, Giacomo and Salviati, Giancarlo and Züttel, Andreas and Riccò, Mauro. Decoration of graphene with nickel nanoparticles: study of the interaction with hydrogen. *J. Mater. Chem. A* (2014) 2(4)1039-1046 The Royal Society of Chemistry, Doi 10.1039/C3TA14127F, <http://dx.doi.org/10.1039/C3TA14127F>
17. N.R. Khalid, E. Ahmed, Zhanglian Hong, Yuewei Zhang, M. Ahmad, Nitrogen doped TiO<sub>2</sub> nanoparticles decorated on graphene sheets for photocatalysis applications, *Current Applied Physics*, V12, 2012, P1485-1492, ISSN 1567-1739, <https://doi.org/10.1016/j.cap.2012.04.019>.
18. Gai, Ke & Qi, Huili & Zhu, Xiulan & Wang, Mingye, Preparation of Ag-Fe<sub>3</sub>O<sub>4</sub> nanoparticles sensor and application in detection of methomyl. *E3S Web of Conferences*. (2019). Doi 118. 01002. 10.1051/e3sconf/201911801002.
19. Solati, Elmira & Tari, Sahar & Dorrani, Davoud., Laser ablation assisted synthesis of graphene/CuO nanocomposite: effect of laser fluence. *Materials Technology*. 37. 1-10. 2022, Doi 10.1080/10667857.2022.2080033.
20. Laura L. Beecroft and Christopher K. Ober. Nanocomposite Materials for Optical Applications. *Beecroft 1997 Nanocomposite MF. ChemInform*. 1997(28). <https://api.semanticscholar.org/CorpusID:196765822>.

21. Ahmed I. Abdel-Salam, M.M. Awad, T.S. Soliman, A. Khalid, The effect of graphene on structure and optical properties of CdSe nanoparticles for optoelectronic application, *Journal of Alloys and Compounds*, V898, 2022, 162946, ISSN 0925-8388, <https://doi.org/10.1016/j.jallcom.2021.162946>
22. Onsi, Romany & Easawi, Khaled & Abdallah, Said & Negm, Sohair & Talaat, Hassan. . Preparation of Silver Nanoparticles Dispersed in Almond Oil Using Laser Ablation Technique. *IOP Materials Science and Engineering*, 2020, 762. 012005. Doi 10.1088/1757-899X/762/1/012005.
23. Solati, Elmira & Tari, Sahar & Dorrnian, Davoud, Laser ablation assisted synthesis of graphene/CuO nanocomposite: effect of laser fluence. *Materials Technology*. 37. 1-10.2022, Doi 10.1080/10667857.2022.2080033.
24. Mysara, Ahmed & Gomaa, Islam & Ghalia, Ahmed & Soliman, T. Investigation of Raman spectrum, structural, morphological, and optical features of Fe<sub>2</sub>O<sub>3</sub> and Fe<sub>2</sub>O<sub>3</sub> /reduced graphene oxide hybrid nanocomposites. *Physica Scripta*. 2022, Doi 97. 10.1088/1402-4896/ac9c38.
25. Abdel-Salam, A. I., Soliman, T. S., Khalid, A., Awad, M. M., and Abdallah, S., Effect of reduced graphene oxide on the structural and optical properties of ZnO nanoparticles, *Materials Letters* vol. 355, Art. no. 135465, 2024. doi:10.1016/j.matlet.2023.135465.
26. Abeer S. Altowyan, Ayman M. Mostafa, Hoda A. Ahmed, Effect of liquid media and laser energy on the preparation of Ag nanoparticles and their nanocomposites with Au nanoparticles via laser ablation for optoelectronic applications, *Optik*, V241, 2021, 167217, <https://doi.org/10.1016/j.ijleo.2021.167217>.
27. Li, P.; Zhu, B.; Li, P.; Zhang, Z.; Li, L.; Gu, Y. A Facile Method to Synthesize CdSe-Reduced Graphene Oxide Composite with Good Dispersion and High Nonlinear Optical Properties. *Nanomaterials* 2019, 9, 957. <https://doi.org/10.3390/nano9070957>
28. Sobhanardakani, Soheil & Jafari, Azadeh & Zandipak, Raziye & Meidanchi, Alireza. Removal of heavy metal (Hg(II) and Cr(VI)) ions from aqueous solutions using Fe<sub>2</sub>O<sub>3</sub>@SiO<sub>2</sub> thin films as a novel adsorbent. *Process Safety and Environmental Protection*. 2018, Doi 120. 348-357. 10.1016/j.psep.2018.10.002.

- 29.** de Lima, A. H., Origin of optical bandgap fluctuations in graphene oxide, European Physical Journal vol. 93, no. 6, Art no. 105, Springer, 2020. doi:10.1140/epjb/e2020-100578-7.
- 30.** Soliman, T. & Gomaa, Islam & Mysara, Ahmed & Ghalia, Ahmed. Fabrication, Structural, Morphological, and Optical Features of Mn<sub>2</sub>O<sub>3</sub> Polyhedron Nano-Rods and Mn<sub>2</sub>O<sub>3</sub>/Reduced Graphene Oxide Hybrid Nanocomposites. Optics & Laser Technology, 2023 ,Doi 161. 109126. 10.1016/j.optlastec2023.109126.
- 31.** Taha, Mohamed & Ghalia, Ahmed & Farid, A. & Abdallah, S. & Soliman, T,Controlling the shell thickness of SiO<sub>2</sub> on TiO<sub>2</sub> NPs: Characterization, linear and nonlinear optical properties. Ceramics International, 2024, Doi 50. 10.1016/j.ceramint.2024.02.011.